SPACE TELESCOPE SCIENCE INSTITUTE
Operated for NASA by AURA

Instrument Science Report STIS 2001-02

STIS Geometric Distortion - SMOV3A tests for CCD, NUV-MAMA and FUV-MAMA

J. R. Walsh, P. Goudfrooij & E. Malumuth
April 2001

ABSTRACT

STIS CCD, FUV-MAMA and NUV-MAMA observations in the globular cluster NGC 2808 were performed with a pattern of POS TARG offsets in order to determine the geometric distortion by measuring the offsets of the same stars at different positions on the detector. This test (proposal 8511) is similar to the one done during Servicing Mission Orbital Verification #2 (SMOV2) for the CCD and FUV-MAMA, but is published here for the first time for the NUV-MAMA. For the CCD, the fit to the distortion shows polynomial coefficients that are quite similar to the SMOV2 results. The original observations for the FUV and NUV-MAMA (visits 52 and 53 respectively) were repeated since only one guide star was used following a guide star acquisition failure for Visits 02 and 03. For the FUV-MAMA the geometric distortion results differ slightly from the SMOV2 ones, with a significantly different X scale; the pattern of distortion is however very similar. The NUV-MAMA distortion field is similar in shape to that of the FUV-MAMA, but the amplitude of the distortion field is slightly larger and can exceed 2 pixels at the detector corners. Coefficients for use in combining dithered images are presented for the three STIS detectors.

Introduction

The proposal 8511 (PI: P. Goudfrooij) was the first dedicated measurement of the geometric distortion of the STIS detectors after the initial verification tests following installation of STIS into HST in February 1997. The technique follows that first succesfully used for

WFPC2: to measure the positions of stars in a globular cluster on many frames with small (known) offsets between each frame. POS TARG commands provide the required small offsets and preserve the same guide stars. Using a globular cluster ensures that there are many stars spread over the detector area with which to determine the local distortion. Data on ω Cen taken during SMOV2 were used for the STIS CCD test (proposal 7131) and NGC 6681 for the FUV-MAMA (proposal 7132). The data were analysed by Eliot Malamuth and reported in two STIS IDT reports (Malamuth, 1997a,b); no data were reported for the NUV-MAMA.

This report details the analysis of data of proposal 8511. The first implementation of this proposal (Visit 01, 02 and 03, 18 January 2000) suffered from a guide star acquisition failure at exposure 02.010 (first exposure of FUV-MAMA) which may also have affected the CCD and NUV-MAMA exposures. The MAMA exposures were repeated (Visits 52 and 53 on 16 February). The Visit 01 CCD exposures were repeated on 28 May 2000 (Visit 61).

Details of Observations

For the CCD observations images in the Clear (50CCD) filter were obtained on a grid with separations of 12.5 arcsec (~ 250 pixels) situated in a uniformly spaced grid around the central (i.e. POS TARG 0,0) position with an additional image at the central position. Table 1 lists the Visit 01 CCD images, the POS TARG offsets, the rms jitter on the HST V2 and V3 axes, and the exposure times; Table 2 lists the same parameters for the Visit 61 CCD data. Figure 1 shows as an example the image of the central position (POS TARG 0,0) of the globular cluster field. For the MAMA observations a more restricted set of positions was taken: two pairs of offsets in the positive and negative X directions and two sets of Y offsets from the 0,0 position. Since MAMA imaging is predominantly performed using filters, we decided to take the FUV-MAMA images using the F25QTZ broad-band filter, while the NUV-MAMA images were taken using the F25CN270 medium-band filter. Table 3 lists the visit 52 FUV-MAMA and Table 4 the NUV-MAMA observations. Figure 2 shows the FUV-MAMA image from the central (POS TARG 0,0) position and Figure 3 the same position for the NUV-MAMA data.

Table 1. Visit 01 CCD Observations

Dataset	POS TARG X (arcsec)	POS TARG Y (arcsec)	V2 Jitter (mas)	V3 Jitter (mas)	Exptime (s)
o60q01010	-18.75	-18.75	3.9	4.4	48
o60q01020	-6.25	-18.75	4.1	4.4	48
o60q01030	6.25	-18.75	4.2	4.6	48
o60q01040	18.75	-18.75	4.3	4.6	48
o60q01050	18.75	-6.25	4.7	4.4	48
o60q01060	6.25	-6.25	4.4	4.3	48
o60q01070	-6.25	-6.25	4.2	4.8	48
o60q01080	-18.75	-6.25	4.4	4.5	48
o60q01090	-18.75	6.25	4.4	4.7	48
o60q010a0	-6.25	6.25	4.0	4.8	48
o60q010b0	6.25	6.25	4.1	4.7	48
o60q010c0	18.75	6.25	4.5	4.8	48
o60q010d0	18.75	18.75	4.2	4.4	48
o60q010e0	6.25	18.75	4.3	4.6	48
o60q010f0	-6.25	18.75	4.3	4.7	48
o60q010g0	-18.75	18.75	4.5	4.6	48
o60q010h0	0.0	0.0	4.5	4.4	48

Table 2. Visit 61 CCD Observations

Dataset	POS TARG X (arcsec)	POS TARG Y (arcsec)	V2 Jitter (mas)	V3 Jitter (mas)	Exptime (s)
o60q61010	-18.75	-18.75	4.3	5.4	48
o60q61020	-6.25	-18.75	4.5	5.2	48
o60q61030	6.25	-18.75	4.5	5.0	48
o60q61040	18.75	-18.75	4.3	5.3	48
o60q61050	18.75	-6.25	4.6	4.9	48
o60q61060	6.25	-6.25	4.5	5.7	48
o60q61070	-6.25	-6.25	4.4	5.2	48
o60q61080	-18.75	-6.25	4.5	5.8	48
o60q61090	-18.75	6.25	4.5	5.6	48
o60q610a0	-6.25	6.25	4.4	5.2	48
o60q610b0	6.25	6.25	4.4	5.2	48

Dataset	POS TARG X (arcsec)	POS TARG Y (arcsec)	V2 Jitter (mas)	V3 Jitter (mas)	Exptime (s)
o60q610c0	18.75	6.25	4.4	5.1	48
o60q610d0	18.75	18.75	4.2	5.0	48
o60q610e0	6.25	18.75	4.2	5.5	48
o60q610f0	-6.25	18.75	4.3	5.5	48
o60q060g0	-18.75	18.75	4.8	5.4	48
o60q610h0	0.0	0.0	4.4	5.7	48

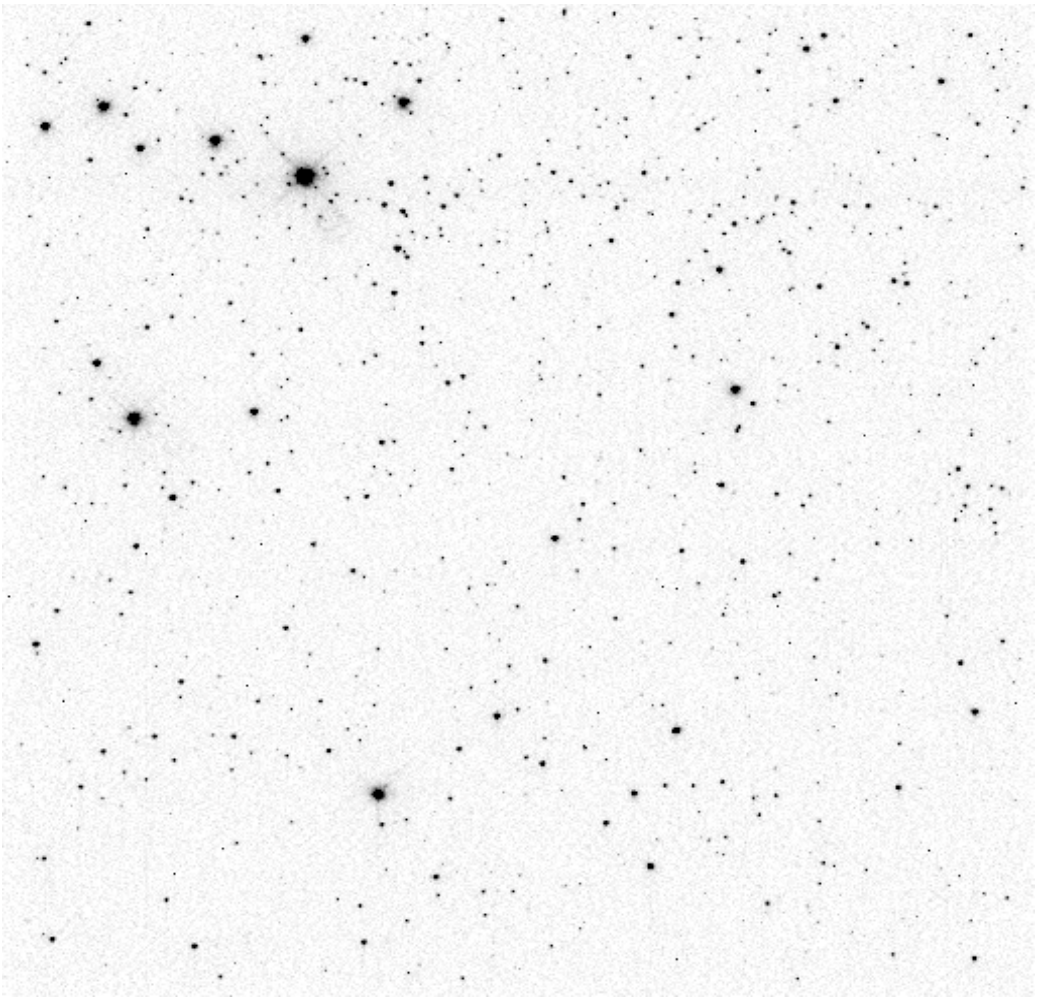

Figure 1: CCD image of central (POS TARG 0,0) position for NGC 2808 (o60q610h0).

Table 3. Visit 52 FUV-MAMA Observations

Dataset	POS TARG X (arcsec)	POS TARG Y (arcsec)	V2 Jitter (mas)	V3 Jitter (mas)	Exptime (s)
o60q52ksq	-10.0	0.0	2.6	4.4	480
o60q52ktq	-5.0	0.0	3.6	5.7	480
o60q52kvq	0.0	0.0	2.6	2.3	480
o60q52kxq	5.0	0.0	3.1	2.4	537.8
o60q52l0q	10.0	0.0	2.3	2.2	480
o60q52l1q	0.0	-10.0	2.6	2.4	500
o60q52l3q	0.0	-5.0	3.6	2.3	500
o60q52l5q	0.0	5.0	2.3	2.1	500
o60q52l7q	0.0	10.0	4.2	2.7	500

Figure 2: FUV-MAMA image of the central position for NGC 2808 (o60q52kvq).

Table 4. Visit 53 NUV-MAMA Observations

Dataset	POS TARG X (arcsec)	POS TARG Y (arcsec)	V2 Jitter (mas)	V3 Jitter (mas)	Exptime (s)
o60q53y5q	-10.0	0.0	3.8	2.1	502
o60q53y6q	-5.0	0.0	3.0	2.4	485
o60q53y8q	0.0	0.0	3.9	2.3	485
o60q53yaq	5.0	0.0	3.0	2.1	485
o60q53ydq	10.0	0.0	3.1	2.6	490
o60q53yeq	0.0	-10.0	2.7	2.2	490
o60q53ygq	0.0	-5.0	2.6	2.3	490
o60q53yiq	0.0	5.0	3.5	2.3	490
o60q53ykq	0.0	10.0	2.4	2.0	536

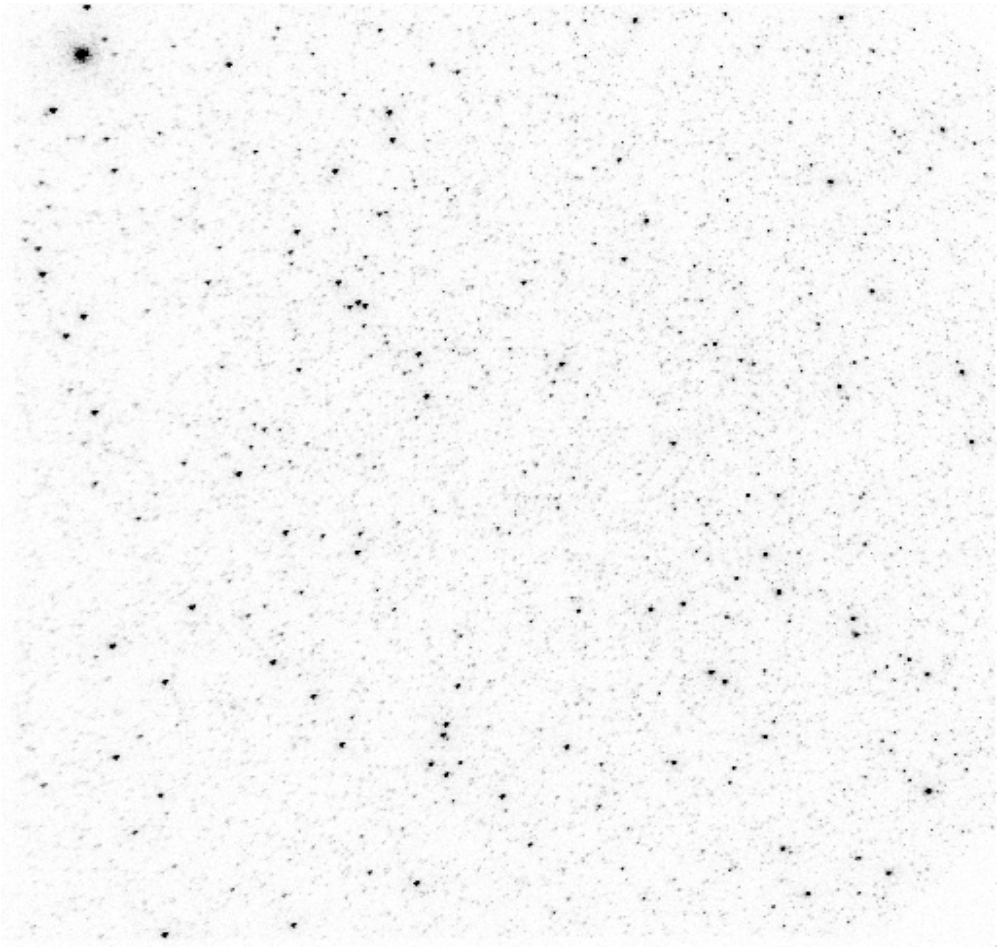

Figure 3: NUV-MAMA image of the central position for NGC 2808 (o60q53y8q).

Basic reductions

For the CCD data all operations were performed on the cosmic-ray-rejected (`*_crj`) products using the pipeline output. For each image at each POS TARG position, daofind (in the noao.digiphot.daophot package) was used to search for stars using a threshold of 120 ADU and a sigma on the background of 3.0. These parameters were chosen after tests and showed that the mean X and Y position errors on running daophot were 0.07 pixels and the average magnitude errors were 0.02 mag. The star positions were recentered in daophot using a Gaussian centering option. For the POS TARG 0,0 image, for example, the number of stars found was 131. The script used to run daofind and daophot for a single CCD image is listed in the Appendix. An ASCII file listing the X and Y positions from daophot and the magnitude and error was used for the subsequent analysis. The image sharpness and roundness were also monitored to check the quality of the star position determination. For the 17 fields a total of 2308 star detections were made.

An essentially identical procedure was performed for the FUV-MAMA and NUV-MAMA images using different parameters. The `*_flt` files were analysed: for the FUV-MAMA the background sigma was 3.0 and the threshold was 40 counts, giving position and magnitude estimates for 95 stars for the POS TARG 0,0 image; whilst for the NUV-MAMA the background sigma was 3.0 and the threshold again 40 counts, producing positions for 167 stars in the POS TARG 0,0 image. The total number of stars measured was 770 for the FUV-MAMA and 1281 for the NUV-MAMA, both in a total of 9 fields.

Shift Analysis

The analysis of the pixel shifts of star images between pairs of POS TARG positions was accomplished in a manner very similar to that described by Malumuth (1997a,b), which was based on the same full third order polynomial fit in X and Y that had been previously employed by the WFPC2 team. The true position (X_T, Y_T) as a function of the observed x-pixel position X and y-pixel position Y is given by:

$$X_T = CC(0) + CC(1)*X + CC(2)*Y + CC(3)*X*X + CC(4)*X*Y + CC(5)*Y*Y + CC(6)*X*X*X + CC(7)*Y*X*X + CC(8)*X*Y*Y + CC(9)*Y*Y*Y \quad (1)$$

$$Y_T = DD(0) + DD(1)*X + DD(2)*Y + DD(3)*X*X + DD(4)*X*Y + DD(5)*Y*Y + DD(6)*X*X*X + DD(7)*Y*X*X + DD(8)*X*Y*Y + DD(9)*Y*Y*Y \quad (2)$$

where the arrays CC and DD are the polynomial coefficients to be calculated, and X and Y are the pixels positions relative to the detector centre (512,512). Although the true position is not known, the “true” offsets between the position of a star on diferent images can be determined from the difference in the POS TARG offsets. However, the POS TARG offsets are not exact, but are subject to typical errors of 0.1% in translation and 0.1 degrees in rotation. Thus whilst the POS TARG values can be used to establish the matching of stars on different images, the ***actual mean pixel offset between frames*** was used as the ‘true’ offset, with which the measured offsets of individual stars can be compared. This holds

provided *(a)* there are many stars in the overlapping region between images and *(b)* the local distortions in the overlap region do not significantly influence the computation of the mean offsets. A FORTRAN program reads all the data files of the positions of the stars from the results of the daophot runs, and the POS TARG offsets between the files. Then the positions of all the stars from one image are compared with all the other stars from the other images using the expected POS TARG offsets to identify the stars in common on other frames. In this way pairs of coordinates are built up which specify the coordinates of the same star on different images together with the POS TARG offsets. In determining the matches, the positions of stars within a few pixels of the position expected from the POS TARG offset are examined and a check is made that the magnitude does not differ by more than one magnitude between the stars in both images in order to avoid spurious matches. As a result of these matches the mean pixel offset between each pair of images is recorded; the mean X and Y pixel scales were determined by comparing those mean pixel offsets with the POS TARG offsets in arcsec. Table 5 lists the mean pixel scales and errors.

Table 5. Mean pixel scales for STIS detectors

Detector	X scale (arcsec/pix)	X scale error (arcsec/pix)	Yscale (arcsec/pix)	Yscale error (arcsec/pix)	Corrected Mean Scale
CCD	0.050716	0.000072	0.050735	0.000087	0.050725
FUV-MAMA	0.024328	0.000025	0.024608	0.000086	0.024468
NUV-MAMA	0.024526	0.000120	0.024829	0.000126	0.024677

A second FORTRAN program then assembled the pairs of X,Y data for the matching stars into a file together with the X,Y offset between these pairs from the mean pixel offsets between frames. This procedure identified 7154 star pairs for the CCD Visit 01 data, 7547 pairs for the CCD Visit 61 data, 1715 for the FUV-MAMA and 2274 for the NUV-MAMA. Figure 4 shows the deviations of the measured X and Y positions from the POS TARG expected positions of all the pairs of star positions for the Visit 61 CCD observations (Table 2). The mean and rms on the X and Y values are indicated on the figure. Figure 5 shows the same plot for the FUV-MAMA and Figure 6 for the NUV-MAMA, referring to the Visit 51 and 52 datasets respectively.

The input data for the solution of the 20 polynomial coefficients in equations (1) and (2) is the file of measured X and Y positions together with the expected positions based on the frame-to-frame shifts. Equation (2) of Malumuth (1997a) provides the offsets (in the sense measured – expected) as a function of the measured offsets and can be solved for the number of star pairs by matrix inversion to yield the 20 unknown coefficients in equations (1) and (2). The IDL procedure of Malumuth (1997a,b) was used to solve for the array of coefficients CC and DD using matrix least squares. Table 6 provides the coefficients of these fits for the CCD, Table 7 for the FUV-MAMA and Table 8 for the NUV-MAMA.

Table 6. Polynomial coefficients of CCD geometric distortion

Coefficient	CC	DD
0	0.0	0.0
1	1.0010598	-1.8546528E-4
2	-2.3369279E-5	1.0006150
3	-2.0376081E-7	8.9324835E-8
4	-2.6036224E-8	2.1104000E-6
5	-2.8393181E-6	-8.0929521E-8
6	-6.0716663E-9	3.0040687E-11
7	1.4334031E-9	-2.7573246E-9
8	-3.1399749E-9	8.0750455E-10
9	7.3569982E-10	-3.1613497E-9

Table 7. Polynomial coefficients of FUV-MAMA geometric distortion

Coefficient	CC	DD
0	0.0	0.0
1	1.0001046	-1.6108220E-4
2	5.0293262E-4	1.0002139
3	5.2875567E-7	9.0029024E-7
4	6.5148835E-6	5.4365430E-7
5	2.4184735E-6	-2.2371567E-6
6	3.2009916E-9	1.2734385E-9
7	3.4281598E-9	-6.4084965E-10
8	-5.5388347E-9	5.4906504E-10
9	4.5507245E-10	-1.2429272E-9

Table 8. Polynomial coefficients of NUV-MAMA geometric distortion

Coefficient	CC	DD
0	0.0	0.0
1	1.0010598	-1.8546528E-4
2	-2.3369279E-5	1.0006150
3	-2.0376081E-7	8.9324835E-8
4	-2.6036224E-8	2.1104000E-6

Coefficient	CC	DD
5	-2.8393181E-6	-8.0929521E-8
6	-6.0716663E-9	3.0040687E-11
7	1.4334031E-9	-2.7573246E-9
8	-3.1399749E-9	8.0750455E-10
9	7.3569982E-10	-3.1613497E-9

Figure 4: Difference of measured and mean image offset X and Y positions for 7154 star ‘pairs’ in the NGC2808 CCD data. Each star ‘pair’ consists of a given star measured in one frame and the same star measured on a frame that was spatially offset from the first frame (using POS TARGs). The mean and rms values are indicated.

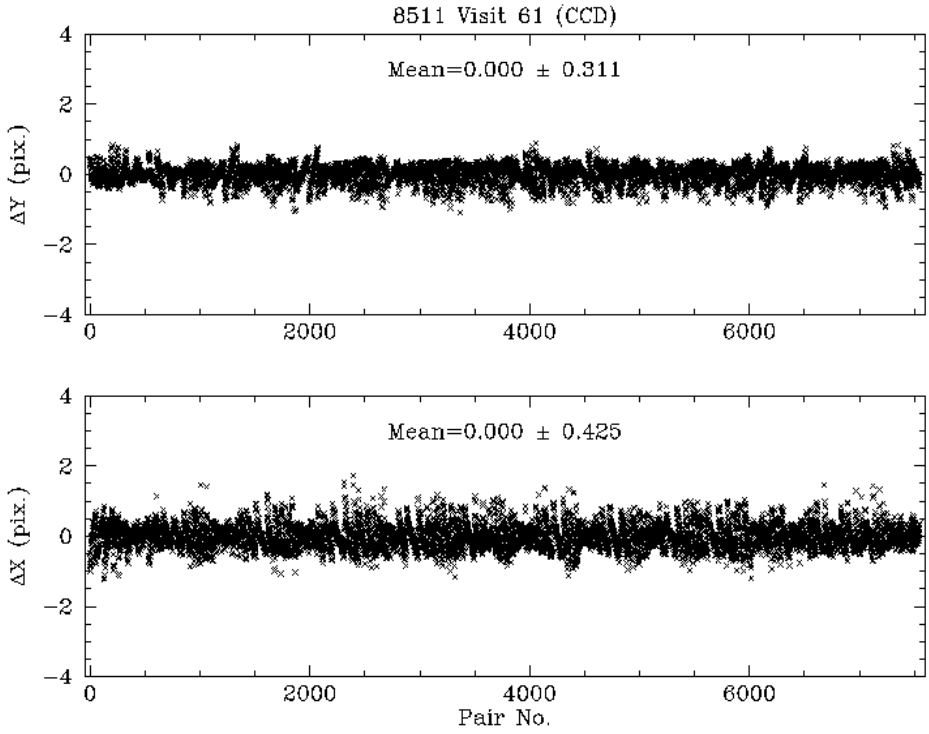

Figure 5: Difference of measured and mean image offset X and Y star positions for 2274 pairs for NGC2808 FUV-MAMA data.

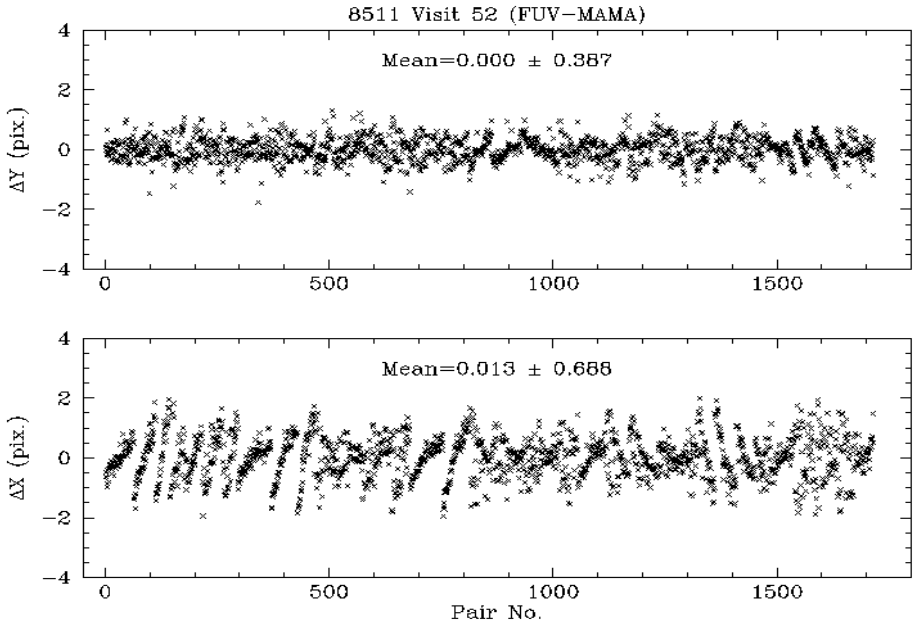

Figure 6: Difference of measured and mean image offset X and Y star positions for 1715 pairs for NGC2808 NUV-MAMA data.

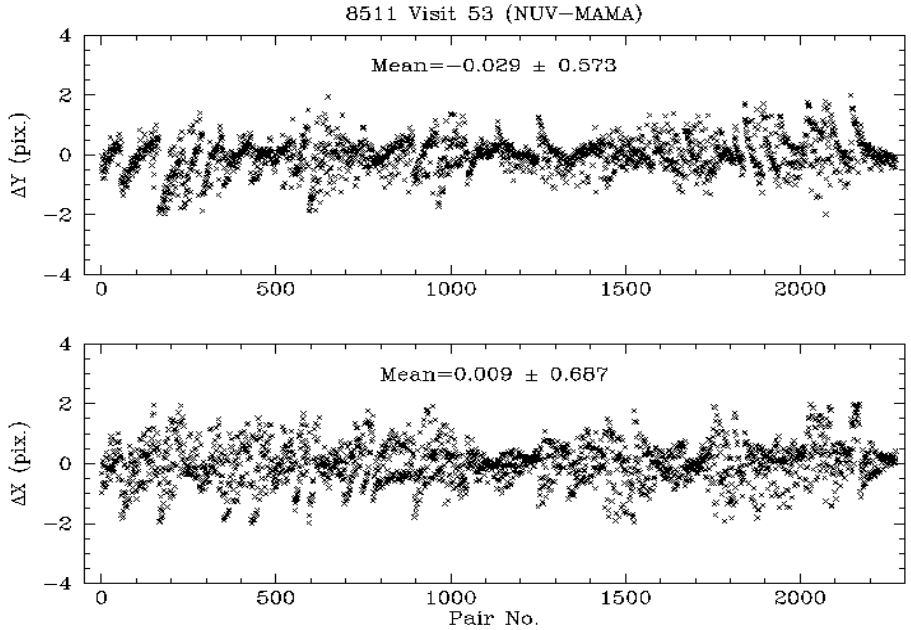

Figure 7: Difference of the polynomial-distortion-predicted X and Y position pairs for NGC 2808 CCD data.

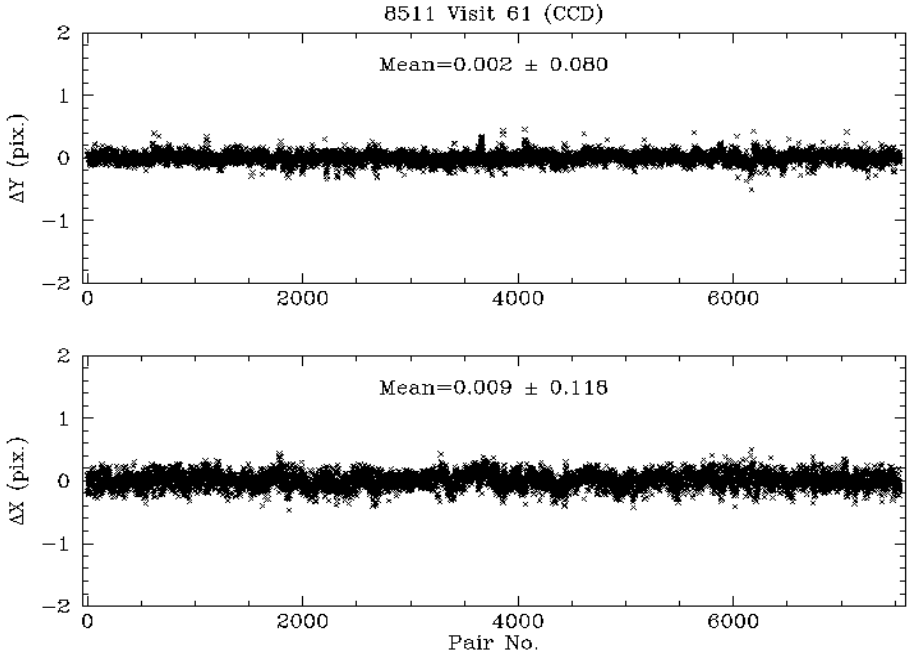

Figure 8: .Difference of the polynomial-distortion-predicted X and Y position pairs for NGC 2808 FUV-MAMA data

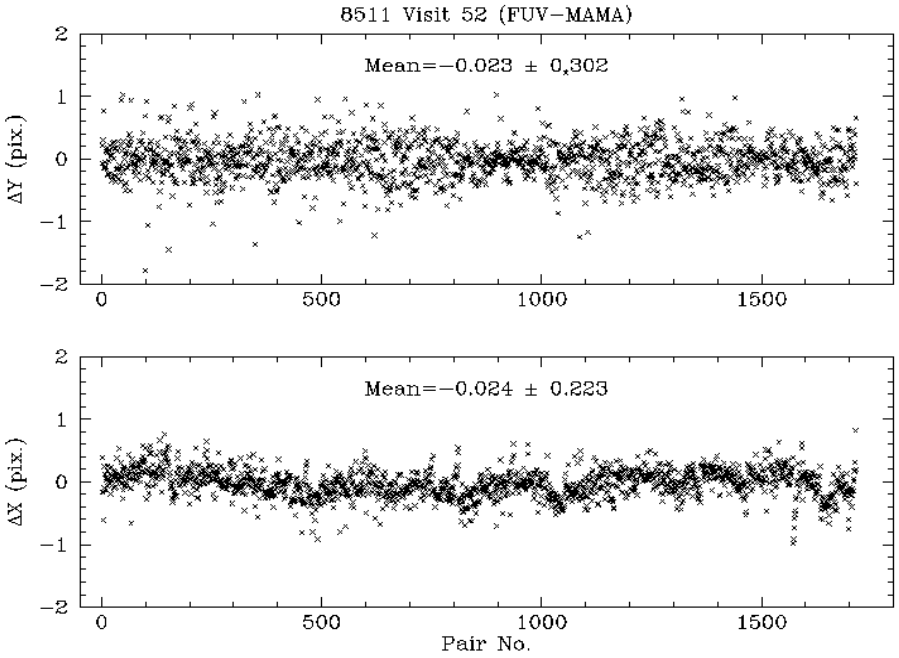

Figure 9: .Difference of the polynomial-distortion-predicted X and Y position pairs for / NGC 2808 NUV-MAMA data.

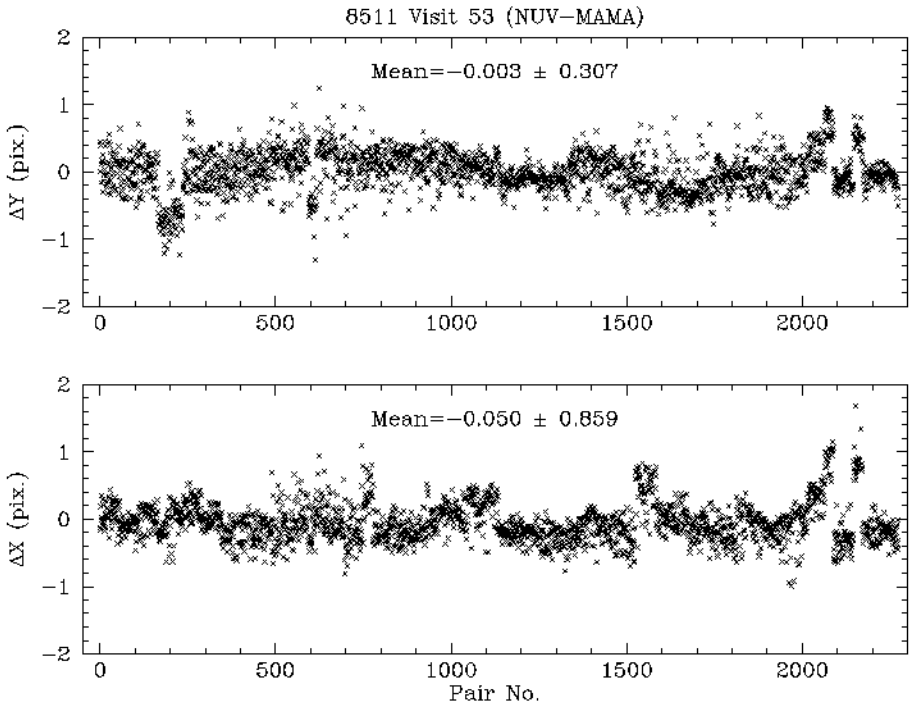

Figure 10: Distortion map for the CCD. Each vector represents the distortion in pixels ∗ 50. The dot shows the undistorted position and the vector the distortion to the observed position

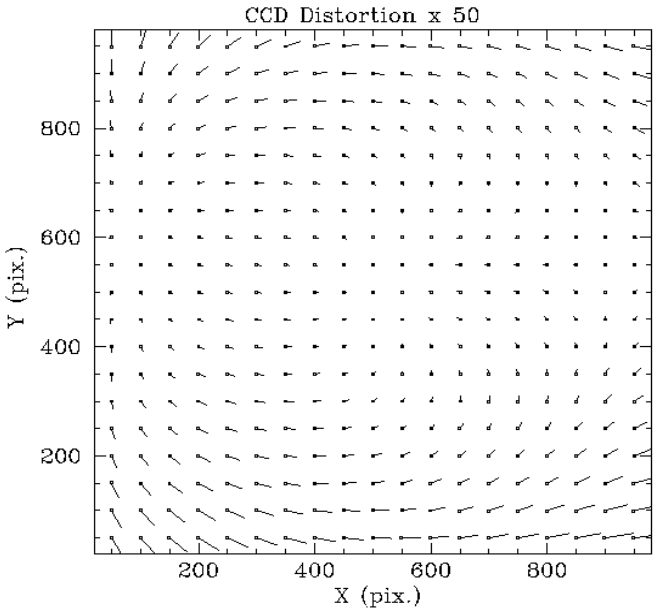

Figure 11: .Distortion map for the FUV-MAMA, with the same notation as Figure 10

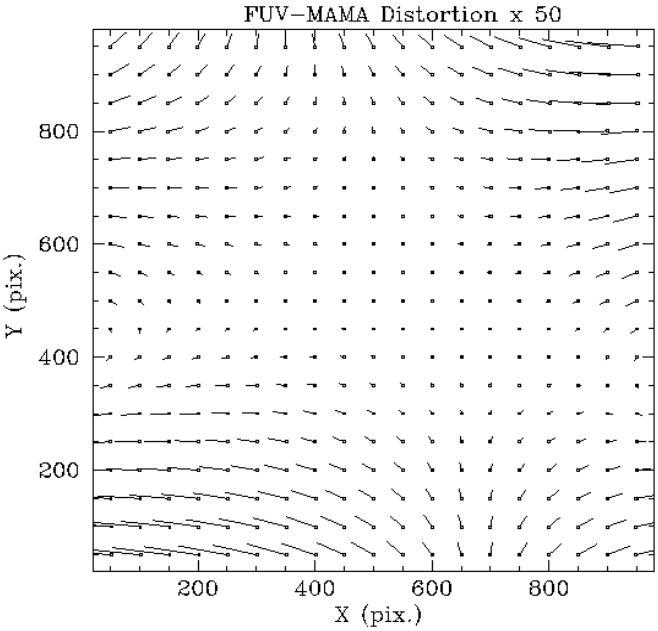

Figure 12: Distortion map for the NUV-MAMA, with the same notation as Figure 10.

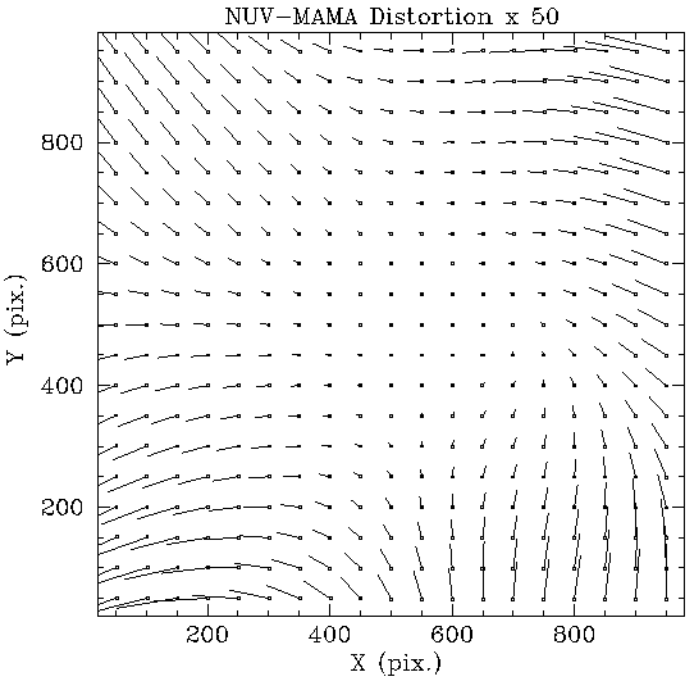

Comparison with SMOV2 Results

The results from the 8511 SMOV3a geometric distortion test can be directly compared with the results from the SMOV2 tests for the CCD and FUV-MAMA. To this end, Table 9 lists the pixel scales given by Malumuth in 1997a (CCD) and 1997b (FUV-MAMA) as well as the corresponding post-SMOV3a numbers from Table 5. For the CCD the results agree to well within the errors; for the FUV-MAMA there appears to have been a change in the X scale, significant at the 5σ level.

Table 9. Comparison of STIS pixel scales from SMOV2 tests with those reported here.

Detector	Servicing Mission	X scale (arcsec/pix)	Yscale error (arcsec/pix)	Yscale (arcsec/pix)	Yscale error (arcsec/pix)	Corrected mean scale
CCD	SMOV2	0.050711	0.000079	0.050726	0.000014	0.050718
	SMOV3a	0.050716	0.000072	0.050735	0.000087	0.050725
FUV-MAMA	SMOV2	0.024465	0.000009	0.024666	0.000018	0.024565
	SMOV3a	0.024328	0.000025	0.024608	0.000086	0.024468
NUV-MAMA	SMOV3a	0.024526	0.000120	0.024829	0.000126	0.024677

The polynomial coefficients in Tables 6 and 7 can also be compared with the SMOV2 results. Figure 13 shows this in graphical form by using the SMOV2 coefficients CC and DD, derived by Malumuth (1997a,b) to correct the SMOV3 Visit 61 data for the CCD and the Visit 52 data for the FUV-MAMA. In comparison with Figure 7 the CCD geometric correction is essentially identical and the rms on the observed and distortion-predicted values are very similar in Figures 7 and 13. For the FUV-MAMA there appears to have been significant change and Figure 14 shows the effect of applying the SMOV2 coefficients CC and DD to the SMOV3a measurements. The effect of the 0.6% change in X scale causes the slope in the X residuals. There is no detectable change in the Y scale. The rms on the residuals is very similar between Figures 7 and 14 implying that there has been no disinct change in the *pattern* of distortion over the three-year interval from SMOV2 to SMOV3a.

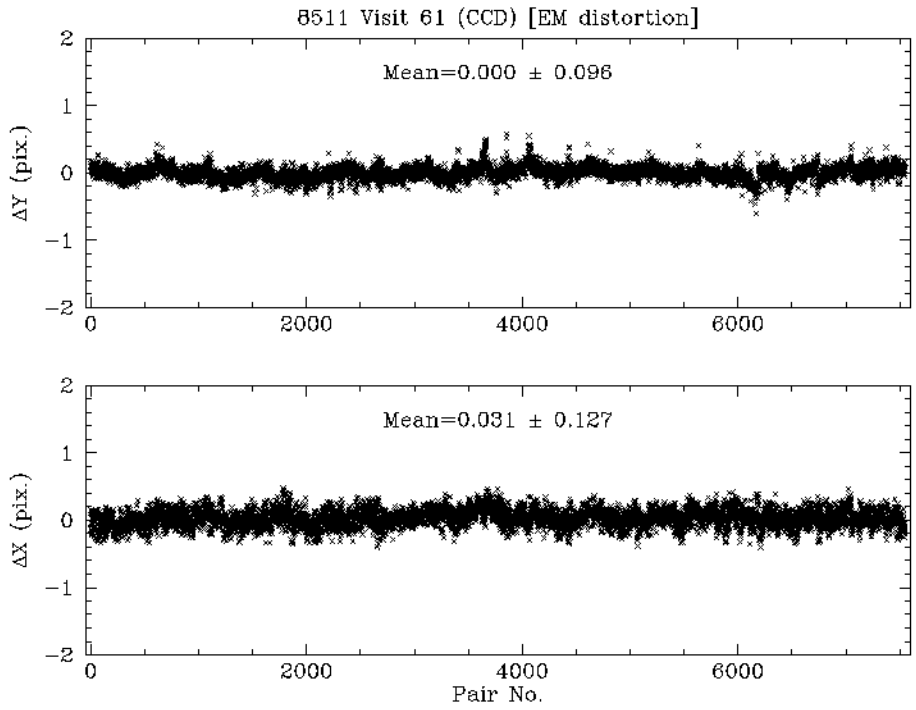

Figure 13: Difference of the polynomial distortion predicted X and Y position pairs for the NGC 2808 CCD data using the CC and DD polynomial coefficients derived by Malamuth (1997a) from the SMOV2 data.

Conclusions

The pixel scale and distortion of the STIS CCD, FUV and NUV-MAMA detectors have been determined during SMOV3a from measurements of a star field in NGC 2808. Table 6 lists the distortion coefficients for the STIS CCD and Tables 7 and 8 for the FUV-MAMA and NUV-MAMA, respectively. These coefficients can be directly used by the stsdas.analysis.dither package in combining dithered STIS images. The coefficients show

no change in CCD scale or distortion over three years since the last test. For the FUV-MAMA there is a small (0.6%) change in X scale detected, but no overall change in the distortion field over the three year interval. For the NUV-MAMA the distortion coefficients are presented for the first time, in Table 8. They show a distortion field that is very similar to the FUV-MAMA but the magnitude of the distortions are slightly larger.

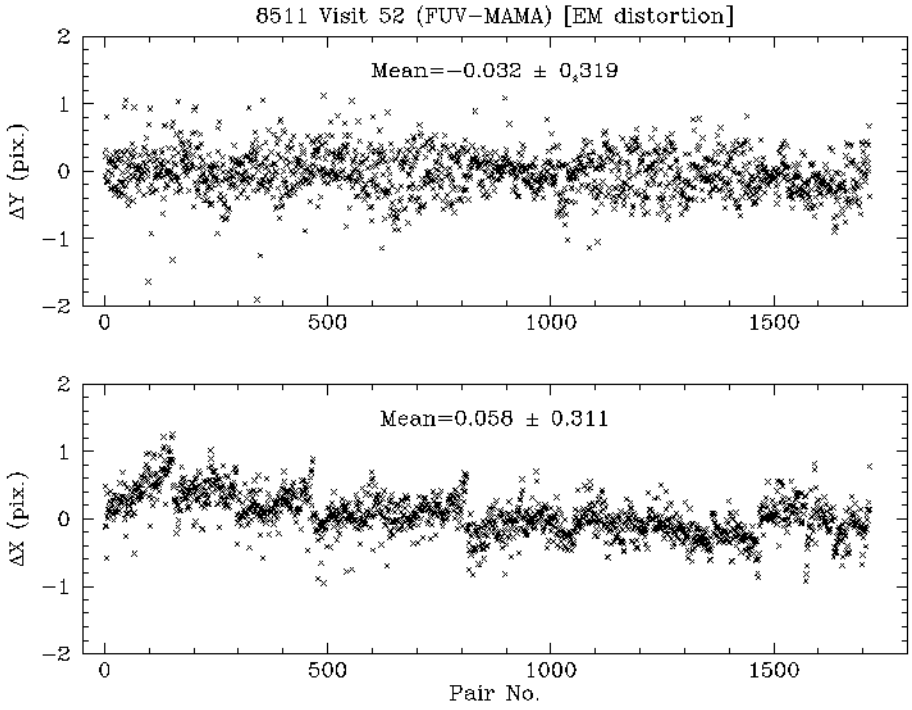

Figure 14: Difference of the polynomial-distortion-predicted X and Y position pairs for the NGC 2808 FUV-MAMA data using the CC and DD polynomial coefficients derived by Malamuth (1997b) from the SMOV2 data.

References

Malumuth, E., 1997a. STIS CCD Geometric Distortion. STIS Post Launch Quick Look Analysis Report No. 33. STIS IDT, Greenbelt.

Malumuth, E., 1997b. STIS FUV-MAMA Geometric Distortion. STIS Post Launch Quick Look Analysis Report No. 41. STIS IDT, Greenbelt.

Appendix. Analysis Procedure

1. Run noao.digiphot.daophot.daofind on each image at each POS TARG position. For the different detectors the parameters were as follows:

CCD sigma=3. nsigma=1.5 threshold =100 readnoi=4.3
FUV-MAMA sigma=3. nsigma=1.5 threshold =40
NUV-MAMA sigma=3. nsigma=1.5 threshold =40

2. Dump X, Y centers, magnitude, sharpness and roundness to ASCII file. The mean and standard deviation of sharpness and roundness were printed to assess the star finding process (e.g. trailing, effect of blending).

3. Run noao.digiphot.daophot.phot on each image using the images found in 1. For all the detectors the aperture was 5 pixels and the offset of the sky annulus 10 pixels. The method to assess the sky background was median. The zero point appropriate to each exposure was set. The centre position was redetermined using a 2D Gaussian fit for the centering algorithm.

4. Display the data frame and mark the photometered stars as a further check on 1 and 3.

5. Dump X, Y centres and X, Y errors, output from 3, to a single ASCII file (using txdump). Dump X, Y centres, magnitude and error to a separate ASCII file. The mean and standard deviation of all the X and Y errors and the mean and standard deviation of the magnitude and magnitude errors were printed to assess the quality of the fitting and photometry. Based on the mean and standard deviation of the centring errors and the photometry errors, the threshold and sigma in step 1 were altered. Typical values of X and Y error were 0.07 pixels for the CCD and 0.06 and 0.05 pixels for the FUV-MAMA and NUV-MAMA respectively. The mean magnitude errors were 0.02 for the CCD and 0.02 and 0.03 for the FUV-MAMA and NUV-MAMA respectively.

6. Form an ASCII file listing the names of the images and the POS TARG X and Y offsets in arcsecs.

7. Run the FORTRAN program comp1 to compare each pair of images, finding the X and Y offsets between the same star on each image pair. The POS TARG offsets between image pairs were used to predict where to search for the star position within 3 pixels of the expected position and requiring that the magnitude of the same star on paired images did not differ by more than 1 magnitude, to further ensure against mis-matches. The output consists of an ASCII file listing the X,Y of each the matched pair, their POS TARG expected X and Y offsets, the mean magnitude and magnitude difference for all the POS TARG positions. In addition an ASCII file of the mean seperation of each image pair based on the actual star positions is output. The mean X and Y pixel scales, determined from the offsets where the POS TARGs are non-zero, are reported (see Table 5).

8. Run FORTRAN program comp2 which is similar to comp1 but now uses the mean pixel offsets between images, from item 7, and outputs, as an ASCII file, the measured X,Y position differences and the expected differences using the mean pixel offsets between different images. This step eliminates the distortion introduced by POS TARG offsets differing from the commanded ones.

9. Plot the output file from 8 with smongo (e.g. Figs. 4-6)

10. Read the output ASCII file from item 8 into arrays in IDL compatible with the fitgeo routines of Malamuth (1997a) and run fitgeo. The CC and DD distortion coefficients (Tables 6-8) are written to an ASCII file.

11. Run FORTRAN program rectifxy which reads in the ASCII file of the distortion coefficients from item 10 and the ASCII file of the measured positions from item 8. The measured points are corrected for distortion, and an output ASCII file lists the distortion-corrected sets of X and Y values together with the expected X and Y differences from the mean pixel offets between image pairs.

12. Plot the output file from item 11 with smongo (e.g. Figs. 7-9)

13. Run FORTRAN program distortplot to plot the distortion field, as parameterized by the distortion coefficients from item 10, calling smongo (e.g. Figs. 10-12).